Journal of Materials Chemistry A

The Importance of Anode Protection towards Lithium Oxygen Batteries

Journal:	*Journal of Materials Chemistry A*
Manuscript ID	TA-REV-11-2019-012414.R1
Article Type:	Review Article
Date Submitted by the Author:	07-Jan-2020
Complete List of Authors:	Bi, Xuanxuan; Argonne National Laboratory, Chemical Science and Engineering Division Amine, Khalil; Argonne National Laboratory, Lu, Jun; Argonne National Laboratory, Chemical Science and Engineering Division

REVIEW

The Importance of Anode Protection towards Lithium Oxygen Batteries

Received 00th January 20xx,
Accepted 00th January 20xx

DOI: 10.1039/x0xx00000x

Xuanxuan Bi,[a] Khalil Amine*[abc] and Jun Lu*[a]

Developing lithium oxygen (Li-O_2) batteries is critical to achieve high energy density in energy storage devices. Benefiting by the low weight of the cathode reagent, oxygen, Li-O_2 batteries possess a high theoretical energy density of 3500 Wh kg^{-1} based on the formation of Li_2O_2. However, they face several challenges from the metal anode, the air electrode, and the unstable electrolyte. Although most studies have focused on the air electrode, the importance of the anode protection should not be neglected. In this review, we aim to understand the challenges on the lithium anode in Li-O_2 batteries, which include Li dendrite growth, parasitic reactions between Li and active species in the electrolyte, and the oxygen crossover effect. Also, recent advances on the Li protection in Li-O_2 batteries will be introduced. This review emphasizes the importance of anode protection especially in an oxygen rich environment and could be a guidance of future development of Li-O_2 batteries.

1. Introduction

Secondary batteries with high volumetric and gravimetric energy densities enable the storage of renewable energies without dissipation. Lithium ion (Li-ion) batteries, as the most popular battery technology, dominate the commercial battery market worldwide. Nevertheless, the high cost and low energy density (387 Wh·kg^{-1}) are major impediments for their applications in electric vehicles (EVs) or large-scale energy storage stations.[1] Lithium air batteries (Li-air) have the potential to provide the energy density of 3500 Wh·kg^{-1} based on the mass of the typical discharge product, lithium peroxide (Li_2O_2), up to nine times higher than that of lithium-ion batteries.[2] This high energy density originates from the active medium in the cathode, oxygen (O_2), and it could be directly obtained from air without reactant storage at the air electrode. The ultimate goal for Li-air batteries is to achieve practical ultrahigh energy density and to be used in the industry with high efficiency and low cost. However, either the practical energy density or the cycle life is far from satisfactory due to the unstable cell environment and the insulating discharge product.[3]

Based on the types of electrolytes and cell configuration, Li-air batteries could be divided into aprotic, aqueous, solid state, and hybrid aprotic/aqueous batteries, among which the aprotic Li oxygen (Li-O_2) batteries have been widely investigated due to their simple cell chemistry and relatively stable cell environment.[4, 5] In an aprotic Li-O_2 battery, the anode, typically Li metal, and the cathode (ultrahigh purity oxygen saturated in porous substrate) are divided by a separator soaked with ether based electrolyte. During discharge, Li is oxidized in the anode to produce Li ions, while at the same time, O_2 is reduced at the cathode. During the reduction of O_2, it is firstly reduced to superoxide (O_2^-), an intermediate that is not thermodynamically stable in an electrochemical cell.[6-8] It would quickly undergo further reduction to produce the peroxide (O_2^{2-}) and then combines with Li^+ to form the final solid product, Li_2O_2, deposited on the porous substrate in the cathode.[9] While during the charging process, Li_2O_2 gets oxidized to release O_2 and Li^+. The electrochemical reactions are listed below.

$$\text{Anode: } Li \leftrightarrow Li^+ + e^- \quad (1)$$

$$\text{Cathode: } 2Li^+ + O_2 + 2e^- \leftrightarrow Li_2O_2 \quad (2)$$

Overall

$$2Li + O_2 \leftrightarrow Li_2O_2 \ (E^0 = 2.96\text{ V, } \mathit{vs.}\ Li^+/Li) \quad (3)$$

The cell chemistry for aprotic Li-O_2 battery is neat but in practical, it faces many challenges. The instability of the Li-O_2 battery derives from nearly all the components in the cell including the anode,[10, 11] the electrolyte,[12] and the cathode[13]. Li metal, as the typical anode material in Li-O_2 batteries, could react with the electrolyte and the trace amount of water in the system to form side products such as LiOH and Li_2CO_3.[14] In addition, O_2 could dissolve in the electrolyte and diffuse to the anode to further react with the Li metal.[10] As for the electrolyte, the typically used salt and solvent in Li-O_2 batteries can be easily attacked by the superoxide species produced during discharge, generating unwanted products and reducing the cycle efficiency.[15, 16] Another issue comes from the insulating discharge product, Li_2O_2.[17] The low electronic and ionic

---

[a] Chemical Sciences and Engineering Division, Argonne National Laboratory, 9700 South Cass Avenue, Lemont, IL 60439, USA
[b] Department of Material Science and Engineering, Stanford University, Stanford, CA 94305, USA
[c] Institute for Research and Medical Consultations (IRMC), Imam Abdulrahman Bin Faisal University (IAU), Dammam, 34212 Saudi Arabia

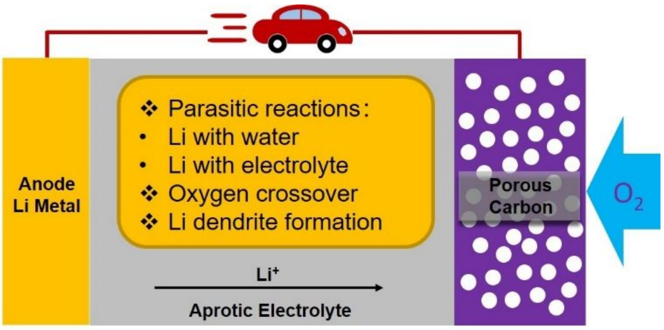

Fig. 1 Schematic diagram of a typical Li-O_2 battery and the issues in the Li metal anode.

conductivities of Li_2O_2 limit the discharge capacity since the accumulation of Li_2O_2 could passivate the substrate and prevent further discharge of the Li-O_2 cell.[18] Moreover, the insulating nature of Li_2O_2 makes it difficult to decompose, leading to an ultrahigh overpotential of over 1 V during charge. Till now, sufficient attentions have been paid on the air electrode and Li_2O_2, since the cathode is the one of the most important limiting factors of the cell stability and cycle life. Numerous studies have been focused on the developing electro-catalysts or redox mediators (RM) to reduce the charge overpotential and improve the energy efficiency.[19-24] However, the role of the anode has not been given due attention.

As the typical anode, Li metal faces many critical problems during the electrochemical cycling. Even though the stability of Li anode has been treated as a severe issue in Li-ion and Li-S batteries, the effect of oxygen crossover in Li-O_2 batteries makes the scenario more complicated.[25] It is very vulnerable to both the electrolyte and the O_2 rich environment because of its highly reductive nature. In this review, we will introduce the challenges existing in the Li metal anode in aprotic Li-O_2 batteries and then focus on the recent advances to improve the stability of the anode materials, such as applying artificial solid-electrolyte-interphase (SEI) layers, solid state membranes, high concentration electrolytes, or replacing the lithium metal to other lithium containing materials. This review could highlight the importance of anode protection and guide the future design of the anode material for Li-O_2 batteries.

2. The importance of anode protection

Different from traditional Li-ion batteries, where the limitation of the capacity results from the host materials in the cathode, much larger capacity could be achieved in Li-O_2 batteries. In this respect, Li metal provides as much as Li source to meet the high capacity. Moreover, it has the lowest electrochemical potential of -3.05 V, making it a good candidate for Li-O_2 batteries.[26] However, the Li anode faces several challenges, illustrated in Fig. 1. The challenges of the Li anode will be discussed in the following section.

2.1 Parasitic reactions of Li and the electrolyte

Impurities in the electrolyte could induce the parasitic reactions in the Li anode. The Li-O_2 battery is an open system where O_2 flows through the cathode. Consequently, water is inevitably included in the gas supply line. Other source of water originates from the trace amount of water in the electrolyte. Water reacts with Li to form LiOH and H_2, following the reaction of $2Li + 2H_2O \rightarrow 2LiOH + H_2\uparrow$.

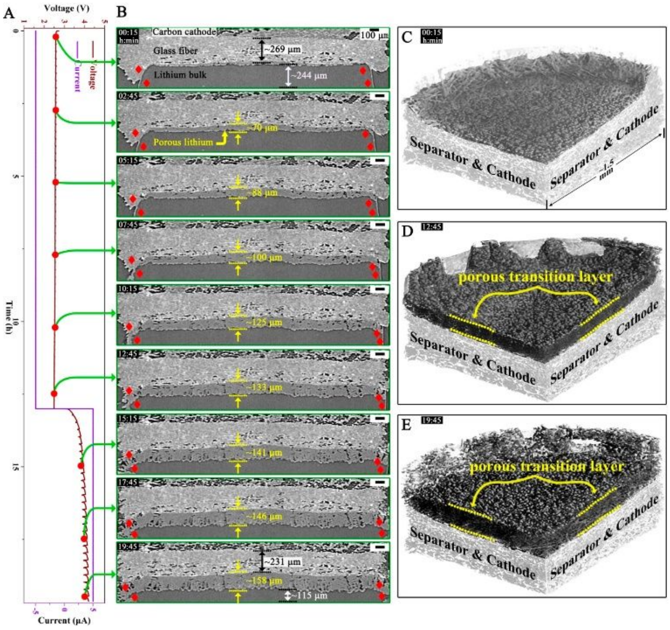

Fig. 2 The evolution of Li surface under the observation of x-ray tomography. (a) Electrochemical cure. (b) Morphological evolution of the LOB during the first discharge–recharge process. Selected 3D demonstrations of the reconstructed data sets shown in panel B with time stamps (C) 00:15, (D) 12:45, and (E) 19:45. Reproduced with permission. Copyright 2018, American Chemical Society.[30]

Another severe issue comes from the reaction of Li and the electrolyte. Generally, Li reacts with the electrolyte to form a compact film that contains the decomposition products and serves as the SEI layer. In a traditional Li-ion battery, the SEI generated from the decomposition reaction of Li and the typical carbonate based electrolyte is relatively stable, which effectively prevents the further direct contact between Li and electrolyte.[27-29] However, in Li-O_2 batteries, the carbonate based solvents are vulnerable to the superoxide species, producing Li_2CO_3 as the irreversible discharge product.[15, 16] Replacing the carbonate based electrolyte by ether based electrolyte, the reversible product (Li_2O_2) is formed, but the SEI on the Li surface becomes more volatile.

Advanced operando techniques were applied in probing the morphology and the growth of the interfaces of Li and the electrolyte. Previous studies showed that multiple side products such as lithium oxides, poly carbonates, and lithium hydroxides were accumulated on the Li anode after cycling. Shui et al. performed synchrotron X-ray diffraction and 3D micro-tomography to visually observe the porous structure on the Li metal anode. They demonstrated that the black colored SEI was composed of mainly LiOH.[14] Similar studies were performed by Sun et al., who used x-ray and neutron tomography to monitor the anode evolution. The morphology change of the lithium anode is shown in Fig. 2.[30] At the beginning of the discharge, a porous-structuralized transition layer starts to grow on the surface of the anode. The transition layer is getting thicker no

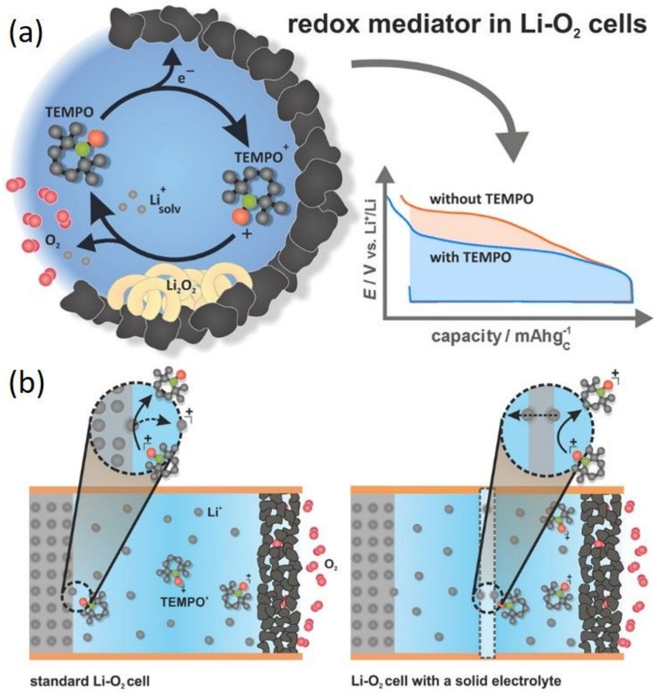

Fig. 3 (a) Schematic representation of the proposed catalytic cycle for the electrochemical charging of Li-O$_2$ cells with TEMPO (left) and the voltage profiles with and without TEMPO (right). Reproduced with permission. Copyright 2014, American Chemical Society.[45] (b) Schematic representation of the possible reactions of redox mediators in aprotic Li–O$_2$ cells without (left) and with (right) a Li$^+$ selective solid electrolyte between cathode and anode. Reproduced with permission. Copyright 2016, American Chemical Society.[47]

matter during the following discharging or charging process, from the top to the bottom in Fig. 2. The results show that the Li continuously reacts with the electrolyte. This irreversible transformation of the Li anode attributes to the decay of the battery by continuously depleting the cell components.

2.2 Oxygen/Superoxide crossover

Li is highly reactive to almost all the components in Li-O$_2$ batteries, not to mention its own issue such as the dendrite formation. In Li-ion batteries, dendrite formation has been considered as a severe safety issue,[31] where the uneven surface of Li generates uneven Li$^+$ distribution, leading to a non-uniform deposition of Li during charge. The persistent Li stripping/plating subsequently leads to the Li dendrite growth, which could penetrate the separator to short the cell.[32] Additionally, Li dendrite breaks the continuous SEI and expose the fresh Li surface to the electrolyte, resulting in continuous Li loss. Although the behavior of Li dendrite has been widely investigated in the field of Li-ion batteries, the scenario in Li-O$_2$ batteries is quite different. Owing to the presence of O$_2$ and superoxides (O$_2^-$), they dissolve in the electrolyte and travel across the separator to the Li anode.[10, 33] In the effect of O$_2$, the growth of Li dendrite could be largely suppressed.[34, 35]

However, more parasitic reactions could be induced by O$_2$. The oxygen crossover effect is firstly recognized by Assary et al. They observed multiple oxidative products on the anode, such as LiOH, Li$_2$CO$_3$, as well as CH$_3$OLi, CH$_3$Li, and polymeric layers.[10] O$_2$ has a profound impact on the formation of solid-electrolyte interface (SEI) layer, attributing to the changes of its composition compared to Li-ion batteries. The direct contact of Li and O$_2$ (dissolved in the electrolyte) may induce the complex electrolyte decomposition, along with the suppression of the Li dendrite growth. Oxygen crossover and the instability of electrolyte have been proved to be one of the major problems for the decay of the Li anode. It is critical to apply a membrane between the anode and cathode to prevent O$_2$ crossover.

2.3 Shuttle effect of redox mediators

The high reactivity of Li anode leads to the parasitic reactions not only with the electrolyte and O$_2$, but also with the additives. Redox mediators (RM) are the typical additive in Li-O$_2$ batteries, since they help to decompose Li$_2$O$_2$ during charge at a lower charge voltage.[36-39] Several redox mediators have been discovered, such as TTF,[37] DBBQ,[23] LiI,[40, 41] LiBr,[42] DMPZ,[39] FePc,[43] or other various chemical compounds. Generally, the redox mediators serve as mobile charge carriers in the local area of the air electrode. During charge, the redox mediator molecules get oxidized at the air electrode to form RM$^+$ by an electrochemical reaction (Equation 4), which subsequently react with Li$_2$O$_2$ through a chemical reaction (Equation 5). The reaction pathway is shown as follows:

$$2RM \rightarrow 2RM^+ + 2e^- \qquad (4)$$

$$2RM^+ + Li_2O_2 \rightarrow 2RM + 2Li^+ + O_2 \qquad (5)$$

Taking 2,2,6,6-tetramethyl-1-piperidinyloxy (TEMPO) as an example, TEMPO$^+$/TEMPO has a standard redox potential of 3.70 V vs. Li$^+$/Li,[44] which reduces the charge potential of Li-O$_2$ batteries from over 4.2 V to ~3.7 V, shown in Fig. 3a.[45] However, in general, the oxidized form of redox mediators, RM$^+$, could diffuse to the Li anode through the electrolyte, generating the redox shuttling effect, which continuously consumes the redox mediator, shown in Fig. 3b, left.[46] Bergner et al. observe the shuttling effect in the TEMPO study and they propose the use of a Li$^+$ selective membrane (LATGP) to divide the anode and the cathode to inhibit the “cross-talk” of both electrodes, shown in Fig. 3b, right.[47] They demonstrate that the LATGP solid electrolyte not only blocks the redox shuttling, but also suppresses the parasitic reactions at the cathode, indicating that the species generated from the Li anode could also promotes the reactions in the cathode. In the report from Ha et al., they notice that the catalytic activity of the redox mediator (10-methylphenothiazine (MPT)) degrades each cycle in Li-O$_2$ batteries. In a symmetric cell, MPT is more stable at an O$_2$ atmosphere compared to Ar, due to the formation of a Li$_2$O layer to prevent the side reaction under O$_2$. However, in a Li-O$_2$ cell, MPT is oxidized to MPT$^+$ in the cathode and then diffuses to the anode to reduce the protecting Li$_2$O layer, accelerating the reaction between MPT and Li, instead.[35]

3. Anode Protection

Given all the issues in the Li anode, it is imperative to find strategies to reduce the reactivity of the anode and improve the cell stability. A variety of approaches has been proposed, such as creating an artificial layer on Li anode, using modified electrolytes, or directly replacing Li metal with other lithium containing composite materials. The implementation of those

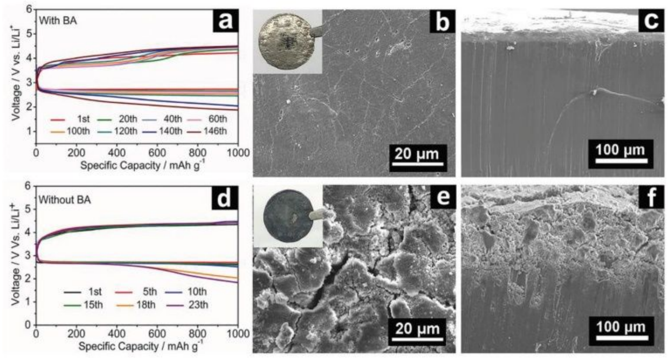

Fig. 4 (a) The voltage profiles of Li-O_2 battery with boric acid. SEM images of the Li foils after 23 cycles with top view (b) and cross-section (c). (d) The voltage profiles of Li-O_2 battery without boric acid. SEM images of the Li foils after 23 cycles with top view (e) and cross-section (f). The insets in (b) and (e) stand for the digital images of the corresponding Li anodes. Reproduced with permission. Copyright 2018, Wiley-VCH.[54]

strategies is considered as key steps in further developing Li-O_2 batteries.

3.1 Building artificial layers by Li surface modification

In the last section, several issues were introduced in Li-O_2 batteries, including the instability of Li metal to the electrolyte, O_2 crossover and the shuttle effect of the redox mediator. In order to solve the issues, creating an artificial layer with decent Li ion conduction could be an effective strategy. The main purpose of the layer is to passivate the surface of Li metal and eliminate the direct contact of Li and the active species. An effective protecting layer should meet the following criteria: (i) it should be stable in the cell environment, (ii) it should have a decent ionic conductivity for Li^+, (iii) it should tolerant the volume change of the Li metal. The strategies to create the artificial layer can be divided into two categories: 1. pretreatment of the Li surface before battery operation; 2. applying additives in the electrolyte to create a stable solid-electrolyte-interphase (SEI) layer during cycling.

3.1.1 Pretreatment of Li metal

Many types of pre-treatments have been performed to modify the Li surface. Fluoroethylene carbonate (FEC) has been proved to be an effective additive in Li-ion batteries, which was also proposed in Li-O_2 batteries. Liu et al. used FEC as a film-forming additive to pre-treat Li metal. With the FEC-treated Li anode and a super P cathode, the Li-O_2 battery runs over 100 cycles at a current density of 300 mAh·g^{-1}, which is much improved compared to the pristine Li metal.[48] They also observe that the amount of LiOH on FEC-treated Li is less than the pristine Li, along with a much cleaner surface after 60 cycles. Another group assembled a Li-O_2 battery with Li metal anode and carbon nanotubes (CNTs), and pre-charged the cell in an Ar atmosphere.[49] Both the Li anode and the cathode were covered by the side products resulted from the decomposition of the salt and solvent. The Li-O_2 battery delivered prolonged cycle life of 110 and 180 cycles under the limited capacity protocol of 1000 mAh·g^{-1} and 500 mAh·g^{-1}, respectively. In another study, a Li/cross-stacking aligned carbon nanotubes anode was applied in Li-O_2 batteries and the cycle life of the battery increased from 50 to over 250 cycles.[50] The artificially built lithium surface layer creates a smooth surface for Li deposition, suppressing the Li dendrite formation and mitigating the anode volume change during cycling.

Zhang et al. introduced a simple method to produce a protective layer by treating Li with 1,4-dioxacyclohexane (DOA), subsequently forming poly(DOA) on the surface of Li.[51] Compared to the pristine Li, the DOA-treated Li anode showed longer cycle life and experienced less surface change. In addition, the parasitic reactions on the anode were suppressed with the modified anode. Liao et al. immersed Li into a $GeCl_4$-THF steam to create a 1.5 μm thick protection layer composed of Ge, GeO_x, Li_2CO_3, LiOH, LiCl, and Li_2O on Li surface. This layer not only protected Li in O_2, but also in up to 45% humidity. More than 150 cycles were obtained in this "moist" Li-O_2 battery.[52] Asadi et al. modified the Li anode with CO_2 gas form a Li_2CO_3/C layer on the surface. This protection layer could make Li survive in an air-like environment over 700 cycles without apparent decay. DFT calculations showed the interface between Li and Li_2CO_3 was relatively stable and it could prevent the penetration of N_2 and O_2.[53] These strategies could effectively extends the life-span of Li metal, resulting in the improvement of the cycle life of the Li-O_2 batteries.

3.1.2 SEI created by electrolyte additives

In addition to pre-forming a stable SEI, the spontaneous generation of SEI with additives in the electrolyte is another approach to protect the Li anode. Huang et al. employed boron acid as an SEI-forming additive in the Li-O_2 battery, creating a continuous SEI with O-B-O bonds linked with Li_2O and LiOH.[54] With boron acid, the cycle life has been largely increased and the surface of Li does not suffer a dramatic change after 23 cycles, shown in Fig. 4a-c. While for the pristine Li, cracks are observed after 23 cycles (Fig. 4d-f), and the surface is covered by the blackish SEI, indicating the formation of LiOH and other side products. Another additive, 2,2,2-trichloroethyl chloroformate (TCCF), was introduced by Wang et al., forming a LiCl-rich SEI layer on the Li metal. With the additive in the electrolyte, the Li-O_2 battery reached 50 cycles at a current density of 100 mA·g^{-1}.

Building an artificial layer is effective in suppressing the side reactions between Li metal and the active species in the electrolyte. However, the mechanism studies on the protecting effect is not sufficient at this stage. Togasaki et al. investigated the influence of the chemical structure of the surface and interior of the SEI. They discovered that the composition of SEI strongly affected the cycling performance of the anode.[55] Compared with organic compounds such as $ROCO_2Li$ and polycarbonate, inorganic compounds such as Li_2CO_3, Li_2O, and LiF in the SEI provided improved protection against side reactions in 1 M LiTFSI/DMSO electrolyte. They suggest that more inorganic compounds should be manipulated in the SEI to improve the cycle efficiency.

From most recent studies, what we can see is that once a stable porous layer is coated on the Li anode, it is expected to be protective from the attacks from the electrolyte, since it reduces the contact area of Li and the electrolyte.[56] Although it is observed that the artificial layers show an apparent improvement compared to the original SEI on Li, the stability of the artificial layer is still questionable in the long run. Moreover, it could also introduce an increased resistance to the cell. More in-depth studies on the artificial layer is needed because it could guide us the rational design of the specific composition of the SEI layer.

3.2 Modification of electrolytes

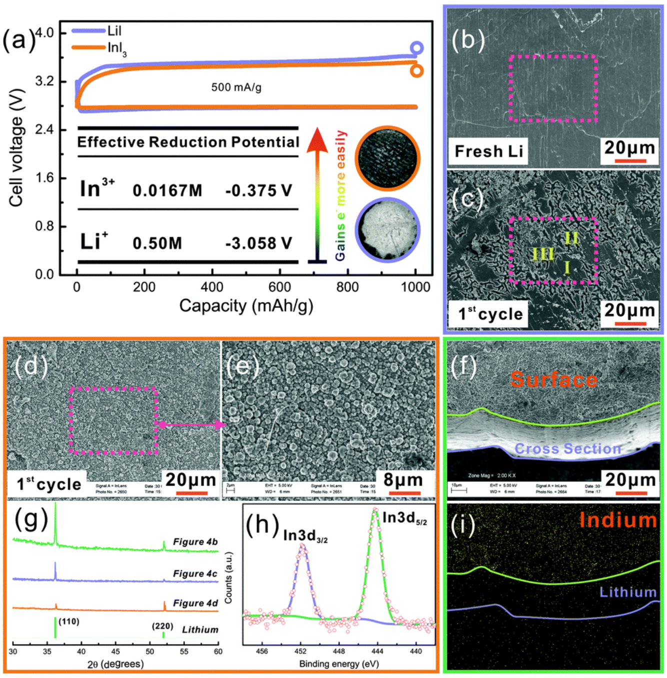

Fig. 5 (a) First cycle voltage profiles of LiI or InI_3 containing $Li-O_2$ coin cell. The inset shows the photographs of the Li surface after the first cycle with InI_3 (top) and with LiI (bottom). Micrograph images of (b) Li anode, (c) Li anode in the LiI after 1st cycle, (d) and (e) Li anode in the InI_3 after 1st cycle, and (f) cross section of the Li anode in the InI_3 after the first cycle. (g) XRD patterns of the fresh Li anode and the Li anodes after the first cycle, corresponding to (b–d). (h) The XPS spectra of the Li anode in the In 3d region. (i) EDX mapping analysis of (f). Reproduced with permission. Copyright 2016, Royal Society of Chemistry.[60]

Since Li is vulnerable to most electrolytes in $Li-O_2$ batteries, modification of the electrolytes could be another effective strategy to stabilize the Li anode. The modification strategies include looking for functionalized salt, replacing the traditional separator by stable Li-ion conductive membranes, increasing the salt concentration to suppress the unwanted side reactions, and applying gel polymer electrolytes or solid-state electrolytes.

3.2.1 Salts and high concentration electrolyte

Back in 2013, a lithium salt, $LiNO_3$ was proved to enable the stabilization of the SEI on the Li anode. The $LiNO_3$ based $Li-O_2$ battery had a cycle life of over 80 cycles at a current density of 0.1 $mA{\cdot}cm^{-2}$.[57] The catalytic effect of the nitrate anion on Li metal was assigned to its reduction to nitrite:

$$2Li + LiNO_3 \rightarrow Li_2O + LiNO_2 \tag{6}$$

The Li_2O containing SEI provides a protection layer on Li metal while the generated nitrite diffuses back to the cathode and gets oxidized to NO_2, serving as a mediator for the oxygen evolution reaction (OER) at ~ 3.6 V.[58] The protecting behaviour on the anode and the catalytic effect of $LiNO_3$ were further supported by Rosy et al.[59] Other redox mediators were also used in the anode protection. Zhang et al. observed the shuttle phenomenon during charge by using LiI RM. They proposed to apply a self-defence RM, InI_3, in the electrolyte, in order to form a much stable indium layer on the Li metal.[60] As shown in Fig. 5a, both LiI and InI_3 containing electrolytes display similar voltage profiles but the surfaces of Li anodes are different. With LiI, the fresh Li changes into 3 domains (Fig. 5b and c) while with InI_3, the SEI contains In and is more uniform and multi-layered (Fig. 5d-i).

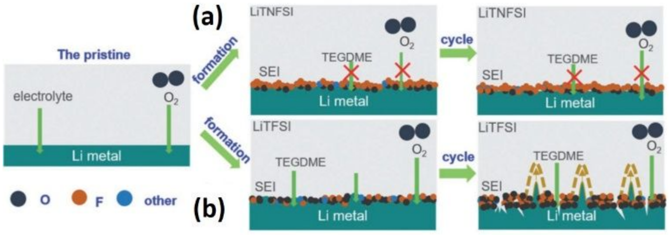

Fig. 6 Schematics depict the reaction and process occurring on the LMA when cycled in (a) LiTNFSI-TEGDME and (b) LiTFSI-TEGDME. Reproduced with permission. Copyright 2018, Wiley-VCH.[61]

They also prove that the In containing SEI not only suppresses the shuttle effect of RM, but also reduce the growth of dendrites.

The salt in the electrolyte also affects the cycling performance of the Li anode. Tong et al. discovered a lithium salt of $Li[(CF_3SO_2)(n\text{-}C_4F_9SO_2)N]$ (LiTNFSI), which effectively reduced the Li dendrite growth, thus enhancing the Coulombic efficiency.[61] The LiTNFSI based electrolyte has a larger electrochemical window than the LiTFSI based electrolyte. They observe higher F contents and less O contents in the SEI for LiTNFSI, where F-rich SEI films are desirable because they are believed to be more flexible and robust. Meanwhile, the less O element indicates that the parasitic side reactions between the LMA and dissolved O_2 are largely suppressed in LiTNFSI/TEGDME, shown in Figure 6. With LiTNFSI, the $Li-O_2$ battery shows a much enhanced reversibility with an O_2 recovery efficiency up to 95.7%.

The electrolyte with a high concentration of salt largely reduces the free solvent molecules, thus eliminating the reaction between the anode and the solvent. Liu et al. investigated the high concentration electrolyte to the performance of $Li-O_2$ batteries.[62] Among 1, 2, and 3 M LiTFSI in DME, they found that the 3 M LiTFSI/DME exhibited the least resistance in O_2 after 40 cycles. The higher concentration electrolyte also demonstrated a much more stable Li anode, along with a stable cyclability. The calculation studies confirmed that less DME free molecules were present and limit the attack from the superoxide species, leading to the increase the stability of the electrolyte. Togasaki et al. compared different concentrations of several salts and discovered that the highly concentrated electrolyte, 4.0 M $LiNO_3$/DMSO, displayed enhanced and stable cycling performance.[63] Zhao et al. added 1,1,2,2-tetrafluoroethyl 2,2,3,3-tetrafluoropropyl ether (TTE) to the 3.4 M LiTFSI/TEGDME electrolyte to make a non-flammable and high concentration electrolyte, which also showed good Li protection effect.[64]

3.2.2 Gel polymer electrolyte and solid-state electrolyte

Given that the traditional liquid electrolytes suffer Li dendrite formation and possible leaking issues, substitution of liquid electrolytes with quasi- or all solid-state electrolytes is benefit for developing a safety battery device. Gel polymer electrolytes (GPEs) have decent ionic conductivity, low cost, and less volatile, which are good alternatives to the traditional liquid electrolyte.

Kim et al. reported a SiO_2-containing gelled quasi-solid-state electrolyte for $Li-O_2$ batteries, in which the hybrid matrix was composed of SiO_2 nanoparticles and polyethylene glycol dimethyl ether (PEGDME).[65] This organic-inorganic matrix had a high Li ion conductivity and improved the discharge capacity of the $Li-O_2$ battery.

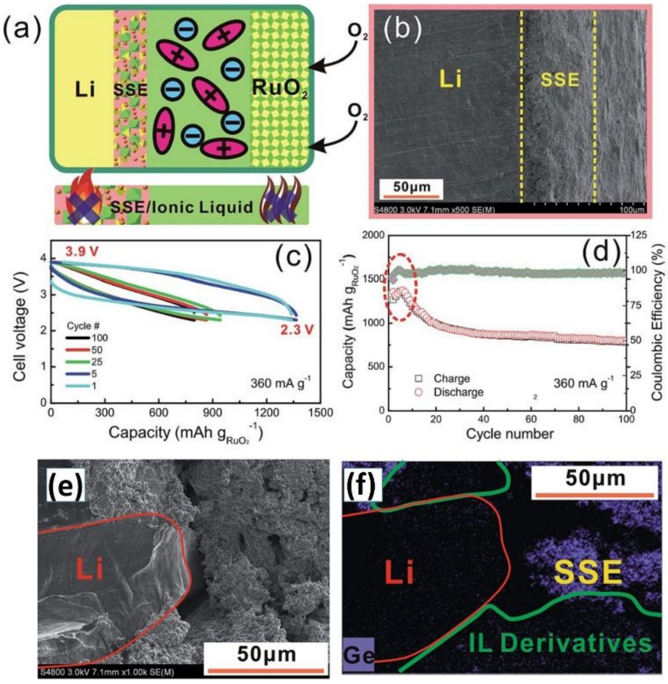

Fig. 7 Electrochemical performance of the IL–SSE-based Li–O$_2$ coin cell with a SSE-modified Li anode. (a) Schematic illustration of the proposed Li–O$_2$ cell. (b) Cross section of the SEM image of the SSE modified Li metal anode. (c) Voltage profiles and (d) cycling profiles and Coulombic efficiency of the Li–O$_2$ cell with a voltage window of 2.3–3.9 V. (e) SEM image and (f) the EDX analysis of the cross section of Li/SSE interface after 100 cycles. Reproduced with permission. Copyright 2018, Royal Society of Chemistry.[85]

They suggested that the binding between SiO$_2$ and PEGDME was favorable to form a gelled electrolyte experimentally and theoretically. Another study reported a TTF-modified quasi-solid-state GPE, a Li-meal-loaded 3D nanoporous graphene anode, and a graphene based cathode for Li-O$_2$ batteries.[66] The GPE was made from mixing silica and PVDF-HFP and soaked in 1 M LiClO$_4$-DMSO with TTF. The GPE suppresses the shuttle effect of TTF and reduces the side reactions in the Li anode. The graphene matrix in the anode also eliminates the Li dendrite growth and accommodates the volume expansion of Li metal.

A composite protective layer (CPL) consisting a composite of Al$_2$O$_3$/PVdF-HFP was employed by Lee et al. on the Li anode in Li-O$_2$ batteries. They also used TEMPO as the redox mediator to observe the protection effect of the CPL from the reaction between the redox mediator and Li metal.[67] It is demonstrated that CPL prevents the reaction between Li and TEMPO$^+$ and improves the Coulombic efficiency of the Li-O$_2$ batteries. Zhao et al. introduced an interconnected nanowire-film-reinforced hybrid GPE (HGPE), serving as both the electrolyte and separator for Li-O$_2$ batteries.[68] MnOOH@Al$_2$O$_3$ skeleton was fabricated, and PVDF-HFP, TEGDME, LiClO$_4$ salt and the LiNO$_3$ were added to the skeleton to form the HGPE. The use of skeleton largely increases the mechanical properties of the film, showing a decent performance for Li dendrite suppression. With high mechanical strength and decent ionic conductivity ($1.04*10^{-3}$ S·cm^{-1} at room temperature), almost 500 cycles were achieved in the Li-O$_2$ batteries.

Although the GPE shows improved protection for Li anode (compared to liquid electrolytes), it still suffers from the issues of limited ionic conductivity and less effective O$_2$ blockage. As another efficient strategy, solid state electrolyte (SSE) only allows Li$^+$ transportation, fully preventing the crossover of other active species from the electrolyte.[69, 70] Generally, the solid inorganic ion conductors for Li ion batteries are selected as alternatives for Li-O$_2$ batteries. Compared to the gel polymer electrolyte, SSE shows much improved stability and better performance at an elevated temperature.

In the presence of SSE, the Li-O$_2$ battery turns to a hybrid cell since it separates the anolyte and catholyte. In this case, the air electrode could also apply air instead of high purity O$_2$. However, when air is used as the cathode reagent, water and CO$_2$ are inevitable to take part in the cathode reactions to form LiOH, LiOH·H$_2$O, and irreversible Li$_2$CO$_3$.[71, 72] Kitaura et al. brought up the issue of the solid state electrolyte, LAGP (Li$_{1.575}$Al$_{0.5}$Ge$_{1.5}$(PO$_4$)$_3$), in air and O$_2$.[73] In air, the humidity in air serves as an ion conductor in the SSE, enabling the cycling of the cell, while in O$_2$, the LAGP suffers more problems, especially at room temperature.[71, 74] Due to the complexity and ambiguity of the air-based Li batteries, we only focus on the pure O$_2$ based cathodes in this review.

Although SSE could serve as a protecting membrane for Li protection, making an all-solid-state Li-O$_2$ battery is challenging. The obstacles are mainly from the interfaces between SSE and the air electrode. Since the solid state discharge product should deposit on the air electrode, the interface between SSE and the air electrode should have enough area of triple phase boundary for product formation. Zhu et al. reduced the thickness of LATP from 600 μm to 36 μm, largely increasing the conductivity of LATP.[75] Moreover, they impregnated LATP to the carbon cathode, making it both electron conductors and catalysts of the cathode for Li-O$_2$ batteries. With such a design, the battery delivered a high discharge capacity of 16800 mAh·g$^{-1}_{carbon}$ at 0.1 mA·cm^{-2} and reached 100 cycles at 6% depth of discharge (DOD) of 1000 mAh·g$^{-1}_{carbon}$. Several other solid state electrolytes have been applied to construct the hybrid Li-O$_2$ batteries, such as NASICON-type Li$_{1+x}$A$_x$Ge$_{2-x}$(PO$_4$)$_3$,[76, 77] Li$_7$La$_3$Zr$_2$O$_{12}$,[78, 79] and Li$_{6.5}$La$_3$Zr$_{1.5}$Ta$_{0.5}$O$_{12}$[80]. Le et al. used aluminium-doped lithium lanthanum titanate (A-LLTO) as the solid electrolyte and LiPON as a protection layer between Li and A-LLZO, Li dendrite growth and electrolyte decomposition are effectively suppressed.[81-84] LiPON was also used in a hexamethylphosphoramide (HMPA) electrolyte to prevent the parasitic reactions between Li and HMPA, leading to a much-improved cycle performance.

In order to achieve both high conductivity and provide a good contact between the electrolyte and the electrodes, hybrid gel polymer/solid state electrolyte was developed. Zhang et al. combined a NASICON ceramic electrolyte (LAGP) and ionic liquid (IL) as the electrolyte (IL-SSE), and RuO$_2$ nanoparticles base cathode, achieving a Coulombic efficiency of 99.5% within 100 cycles, shown in Fig. 7.[85] The SEM in Fig. 7e and 7f shows the distribution of the interfaces between Li, IL, and SSE. As can be seen, although Li loses the contact to the SSE during cycling, IL fills into the voids to maintain the continuous Li$^+$ transport through the interface. Liu et al. employed a hybrid solid electrolyte (HSE) membrane, which was composed of inorganic Li$_7$La$_3$Zr$_2$O$_{12}$ particles and PVDF-HFP both as electrolyte and separator, and a Co$_3$O$_4$-nanowires cathode for Li-O$_2$ batteries. The battery showed comparable discharge capacity compared to the liquid electrolyte based Li-O$_2$ battery and has a cycle life over 200 cycles.[86]

Besides the additives and tuning the salt in the electrolyte, suitable separators are also helpful for increasing the cycle efficiency of the Li

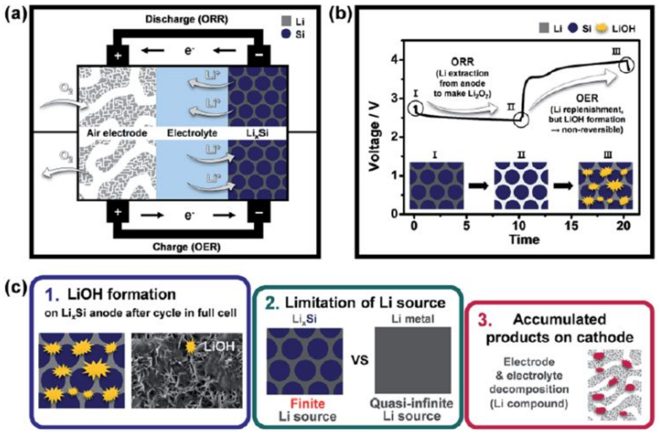

Fig. 8 Schematic images for the discussion of pre-lithiated anode based Li–O_2 full-cell. (a) The system of the Li_xSi-CNT/O_2 full-cell, (b) LiOH formation during the cycling test, and (c) major issues for the Li-O_2 full-cell related to Li loss. Reproduced with permission. Copyright 2016, Royal Society of Chemistry.[93]

anode. For example, several separator alternatives have been applied in Li-O_2 batteries such as Li^+ selective Nafion membranes,[87] Nafion-PEO-graphene membrane,[88] polyurethane/SiO_2/glass fiber nanocomposite separator,[89] and $Cu_3(BTC)_2$ (HKUST-1), a MOF-based separator.[90] Compared to the typical glass fiber based separator, these separators with more compact structure and decent ionic conductivity effectively reduce the crossover of O_2 and redox mediators and block lithium dendrite penetration.

Developing hybrid Li-O_2 batteries with solid state electrolyte is still at an early stage. Solid state electrolyte usually possesses limited ionic conductivity at room temperature, high cost, and fragile. Moreover, the poor interfaces between the Li and the solid electrolyte is an obstacle for obtaining a long life Li-O_2 battery. Most solid state electrolytes are vulnerable to the Li dendrite, which could break the membrane and eventually short the cell. More studies are required to seek for a stable solid state electrolyte for Li-O_2 batteries.

3.3 Composite anodes

Another strategy to improve the stability of the anode is to replace the Li metal anode by other lithium containing materials, such as pre-lithiated carbon materials, or composite materials such as Li_xM_y alloy. They usually have a higher stability than the Li metal, providing a more stable cell environment.

Hirshberg et al. did a preliminary study on pre-lithiated hard carbon anode. They selected hard carbon, instead of graphite or soft carbon to avoid the co-intercalation of the ether solvent into the ordered carbon structures.[91] It was demonstrated that Li_2O_2 is the discharge product but the cells still failed due to the side reactions occurred during the Li^+ intercalation into the carbon matrix. LiOH, and several carbonyl containing moieties are observed on the hard carbon anode, along with the exfoliation of the hard carbon, indicating an unstable interfaces of hard carbon. However, Guo et al. reported a lithium metal carbon nanotube (Li-CNT) anode, where Li was inserted into a porous carbon nanotube matrix and modified by octadecylphosphonic acid for forming an artificial SEI.[92] This Li-CNT anode has almost no volume expansion after cycles and has limited Li dendrite. Moreover, the artificial SEI prevents the parasitic reactions from the electrolyte. Although the cost of the carbon based anodes could be largely reduced but the discharge capacity is restricted, which is comparable to Li-ion batteries but far from satisfactory in metal air batteries.

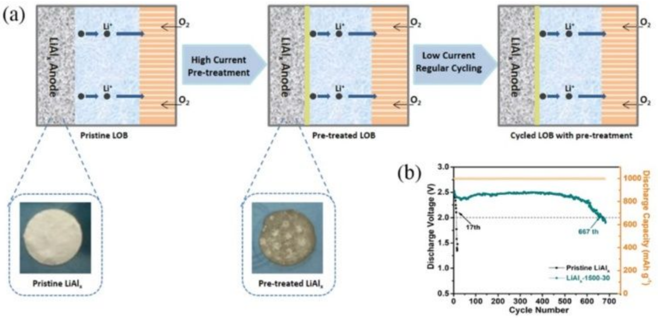

Fig. 9 (a) Schematic illustration of the Li–O_2 batteries with $LiAl_x$ anode subjected to in situ pretreatment process at high current density before regularly cycling at low current density. (b) Cycling performance of pretreated Li-O_2 battery compared with the pristine cell without pretreatment. Reproduced with permission. Copyright 2019, American Chemical Society.[94]

Without the pre-lithiation process, Li alloy becomes a good candidate for replacing the Li anode. Kwak et al. used a lithiated silicon–carbon nanotube composite (Li_xSi-CNT) anode in a full Li-O_2 battery and investigated its stability and the contributed capacity, shown in Fig. 8.[93] The half Li_xSi-CNT cell (vs. Li) delivers a capacity of 1913 mAh·g^{-1}, while the full Li-O_2 cell (Li_xSi-CNT vs. O_2) has a capacity of 1653 mAh·g^{-1} with capacity loss in the presence of O_2. They also observed the formation of LiOH on the Li_xSi-CNT anode during Li replenishment in the full cell, which dramatically reduced the lithium source, resulting in a poor cycle life (Fig. 8b). Hence, Li_xSi has limited Li source compared to the pure Li metal and suffers huge Li source loss during cycles at both the anode (LiOH formation) and the cathode (Li containing side products), shown in Fig. 8c. Guo et al. designed a pre-cycled $LiAl_x$ anode with a stable SEI and only 0.2 *wt* % Al content in Li-O_2 batteries, achieving a long cycle life of 667 cycles, shown in Fig. 9. After the pretreatment, the SEI is confirmed to contain mainly $ROCO_2Li$, Li_2CO_3, LiOH, LiF, and Al_2O_3. The stable and thin Al_2O_3-containing SEI layer could effectively protect the $LiAl_x$ from the side reaction.[94]

4. Summary and future perspective

Analytical measurements have shown the parasitic reactions on the Li metal, contributed to the irreversible change on the anode, resulting in the continuous loss of the anode material in Li-O_2 batteries. Many works have been done to address the issues of the Li anode including building an artificial layer on the surface of Li metal, modification on the electrolyte, applying a solid state membrane, or replacing the Li metal by other Li-containing materials (Fig. 10). These efforts have

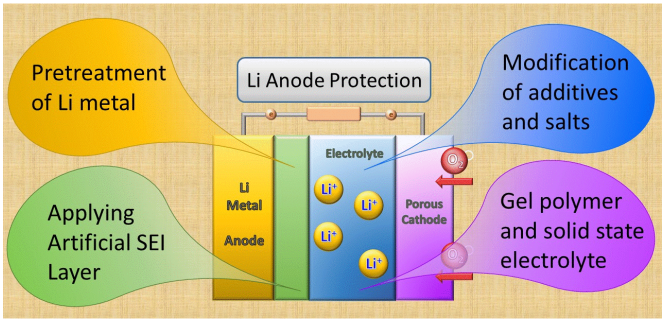

Fig. 10 The schematic diagram of the strategies for Li anode protection.

shown improvements on preventing the parasitic reactions. However, it still requires fundamental investigations of the degradation of Li metal and how the strategies work for improving the stability of Li.

(1) A clear understanding of the Li degradation mechanism is necessary. Unlike the reactions in Li-ion batteries, where the parasitic reactions on the Li anode are mainly attributed to the Li and electrolyte, the reactions in Li-O_2 batteries are more complicated due to the presence of O_2. Several studies have detected multiple side products on the anode and proposed possible decomposition mechanisms between Li, O_2, and the electrolyte, in-depth studies must be conducted to fully understand the side reactions.

(2) In the absence of a stable electrolyte, an artificial layer or a Li selective membrane are extremely important to protect the Li metal. However, although most studies reported the enhancement of the cycle performance of the anode after employing an artificial layer, the underlying mechanism and the role of the layer were still unknown. Why do those strategies could protect Li from reacting with other active species? This is a key question that needs to be addressed in the further development of high efficient protecting layer. In addition, looking for a proper membrane is also challenging because most membranes are fragile, difficult to synthesize, high cost, and has low lithium ion conductivity.

(3) Seeking for a stable electrolyte. Based on previous studies, all the salt and solvents in the electrolyte are reactive to the Li metal, as well as the air electrode. Therefore, looking for a stable electrolyte is always an essential problem for improving the cycle efficiency of the anode and the life span of the full cell.

Conflicts of interest

There are no conflicts to declare.

Acknowledgements

This work is supported by the U.S. Department of Energy (DOE), Office of Energy Efficiency and Renewable Energy, Vehicle Technologies Office. Argonne National Laboratory is operated for DOE Office of Science by UChicago Argonne, LLC, under contract number DE-AC02-06CH11357.

References

1. J. B. Goodenough and K. S. Park, *J. Am. Chem. Soc.*, 2013, **135**, 1167-1176.
2. Y.-C. Lu, B. M. Gallant, D. G. Kwabi, J. R. Harding, R. R. Mitchell, M. S. Whittingham and Y. Shao-Horn, *Energy Environ. Sci.*, 2013, **6**, 750-768.
3. D. Aurbach, B. D. McCloskey, L. F. Nazar and P. G. Bruce, *Nature Energy*, 2016, **1**, 16128.
4. J. Lu, L. Li, J. B. Park, Y. K. Sun, F. Wu and K. Amine, *Chem. Rev.*, 2014, **114**, 5611-5640.
5. D. Geng, N. Ding, T. S. A. Hor, S. W. Chien, Z. Liu, D. Wuu, X. Sun and Y. Zong, *Adv. Energy Mater.*, 2016, **6**, 1502164.
6. J. Lu, Y. J. Lee, X. Luo, K. C. Lau, M. Asadi, H. H. Wang, S. Brombosz, J. Wen, D. Zhai, Z. Chen, D. J. Miller, Y. S. Jeong, J. B. Park, Z. Z. Fang, B. Kumar, A. Salehi-Khojin, Y. K. Sun, L. A. Curtiss and K. Amine, *Nature*, 2016, **529**, 377-382.
7. D. Zhai, K. C. Lau, H. H. Wang, J. Wen, D. J. Miller, J. Lu, F. Kang, B. Li, W. Yang, J. Gao, E. Indacochea, L. A. Curtiss and K. Amine, *Nano Lett.*, 2015, **15**, 1041-1046.
8. N. Mahne, O. Fontaine, M. O. Thotiyl, M. Wilkening and S. A. Freunberger, *Chem. Sci.*, 2017, **8**, 6716-6729.
9. L. Luo, B. Liu, S. Song, W. Xu, J. G. Zhang and C. Wang, *Nat. Nanotechnol.*, 2017, **12**, 535-539.
10. R. S. Assary, J. Lu, P. Du, X. Luo, X. Zhang, Y. Ren, L. A. Curtiss and K. Amine, *ChemSusChem*, 2013, **6**, 51-55.
11. H. Kim, G. Jeong, Y. U. Kim, J. H. Kim, C. M. Park and H. J. Sohn, *Chem. Soc. Rev.*, 2013, **42**, 9011-9034.
12. M. Balaish, A. Kraytsberg and Y. Ein-Eli, *Phys. Chem. Chem. Phys.*, 2014, **16**, 2801-2822.
13. B. D. McCloskey, A. Speidel, R. Scheffler, D. C. Miller, V. Viswanathan, J. S. Hummelshoj, J. K. Norskov and A. C. Luntz, *J. Phys. Chem. Lett.*, 2012, **3**, 997-1001.
14. J. L. Shui, J. S. Okasinski, P. Kenesei, H. A. Dobbs, D. Zhao, J. D. Almer and D. J. Liu, *Nat. Commun.*, 2013, **4**, 2255.
15. B. D. McCloskey, D. S. Bethune, R. M. Shelby, G. Girishkumar and A. C. Luntz, *J. Phys. Chem. Lett.*, 2011, **2**, 1161-1166.
16. S. A. Freunberger, Y. Chen, Z. Peng, J. M. Griffin, L. J. Hardwick, F. Barde, P. Novak and P. G. Bruce, *J. Am. Chem. Soc.*, 2011, **133**, 8040-8047.
17. Y. Zhang, Q. Cui, X. Zhang, W. C. McKee, Y. Xu, S. Ling, H. Li, G. Zhong, Y. Yang and Z. Peng, *Angew. Chem. Int. Ed.*, 2016, **55**, 10717 –10721.
18. V. Viswanathan, K. S. Thygesen, J. S. Hummelshoj, J. K. Norskov, G. Girishkumar, B. D. McCloskey and A. C. Luntz, *J. Chem. Phys.*, 2011, **135**, 214704.
19. M. M. Ottakam Thotiyl, S. A. Freunberger, Z. Peng, Y. Chen, Z. Liu and P. G. Bruce, *Nat. Mater.*, 2013, **12**, 1050-1056.
20. D. M. Itkis, D. A. Semenenko, E. Y. Kataev, A. I. Belova, V. S. Neudachina, A. P. Sirotina, M. Havecker, D. Teschner, A. Knop-Gericke, P. Dudin, A. Barinov, E. A. Goodilin, Y. Shao-Horn and L. V. Yashina, *Nano Lett.*, 2013, **13**, 4697-4701..
21. R. Black, J. H. Lee, B. Adams, C. A. Mims and L. F. Nazar, *Angew. Chem. Int. Ed. Engl.*, 2013, **52**, 392-396.
22. J. Xie, X. Yao, Q. Cheng, I. P. Madden, P. Dornath, C. C. Chang, W. Fan and D. Wang, *Angew. Chem. Int. Ed. Engl.*, 2015, **54**, 4299-4303.
23. X. Gao, Y. Chen, L. Johnson and P. G. Bruce, *Nat. Mater.*, 2016, **15**, 882-888.
24. K. X. Wang, Q. C. Zhu and J. S. Chen, *Small*, 2018, **14**, e1800078.
25. X. Yao, Q. Dong, Q. Cheng and D. Wang, *Angew. Chem. Int. Ed. Engl.*, 2016, **55**, 11344-11353.
26. D. Lin, Y. Liu and Y. Cui, *Nat. Nanotechnol.*, 2017, **12**, 194-206.
27. E. Peled and S. Menkin, *J. Electrochem. Soc.*, 2017, **164**, A1703-A1719.
28. M. Winter, J. O. S. Besenhard, Michael E. and P. Novμk, *Adv. Mater.*, 1998, **10**, 725-763.
29. J. O. Besenhard, M. Winter, J. Yang and W. Biberacher, *J. Power Sources*, 1995, **54**, 228-231.

30. F. Sun, R. Gao, D. Zhou, M. Osenberg, K. Dong, N. Kardjilov, A. Hilger, H. Markötter, P. M. Bieker, X. Liu and I. Manke, *ACS Energy Lett.*, 2018, **4**, 306-316.
31. W. Xu, J. Wang, F. Ding, X. Chen, E. Nasybulin, Y. Zhang and J.-G. Zhang, *Energy Environ. Sci.*, 2014, **7**, 513-537.
32. D. Aurbach, E. Zinigrad, Y. Cohen and H. Teller, *Solid State Ionics*, 2002, **148**, 405– 416.
33. V. Esfahanian, M. T. Dalakeh and N. Aghamirzaie, *Applied Energy*, 2019, **250**, 1356-1365.
34. Y. Kim, D. Koo, S. Ha, S. C. Jung, T. Yim, H. Kim, S. K. Oh, D. M. Kim, A. Choi, Y. Kang, K. H. Ryu, M. Jang, Y. K. Han, S. M. Oh and K. T. Lee, *ACS Nano*, 2018, **12**, 4419-4430.
35. S. Ha, Y. Kim, D. Koo, K.-H. Ha, Y. Park, D.-M. Kim, S. Son, T. Yim and K. T. Lee, *J. Mater. Chem. A*, 2017, **5**, 10609-10621.
36. D. Wang, X. Mu, P. He and H. Zhou, *Materials Today*, 2019, **26**, 87-99.
37. Y. Chen, S. A. Freunberger, Z. Peng, O. Fontaine and P. G. Bruce, *Nat. Chem.*, 2013, **5**, 489-494.
38. D. Kundu, R. Black, B. Adams and L. F. Nazar, *ACS Cent. Sci.*, 2015, **1**, 510-515.
39. H.-D. Lim, B. Lee, Y. Zheng, J. Hong, J. Kim, H. Gwon, Y. Ko, M. Lee, K. Cho and K. Kang, *Nat. Energy*, 2016, **1**, 3926-3931.
40. W.-J. Kwak, D. Hirshberg, D. Sharon, H.-J. Shin, M. Afri, J.-B. Park, A. Garsuch, F. F. Chesneau, A. A. Frimer, D. Aurbach and Y.-K. Sun, *J. Mater. Chem. A*, 2015, **3**, 8855-8864.
41. H. D. Lim, H. Song, J. Kim, H. Gwon, Y. Bae, K. Y. Park, J. Hong, H. Kim, T. Kim, Y. H. Kim, X. Lepro, R. Ovalle-Robles, R. H. Baughman and K. Kang, *Angew. Chem. Int. Ed. Engl.*, 2014, **53**, 3926-3931.
42. Z. Liang and Y. C. Lu, *J Am Chem Soc*, 2016, **138**, 7574-7583.
43. D. Sun, Y. Shen, W. Zhang, L. Yu, Z. Yi, W. Yin, D. Wang, Y. Huang, J. Wang, D. Wang and J. B. Goodenough, *J. Am. Chem. Soc.*, 2014, **136**, 8941-8946.
44. B. J. Bergner, C. Hofmann, A. Schurmann, D. Schroder, K. Peppler, P. R. Schreiner and J. Janek, *Phys. Chem. Chem. Phys.*, 2015, **17**, 31769-31779.
45. B. J. Bergner, A. Schurmann, K. Peppler, A. Garsuch and J. Janek, *J. Am. Chem. Soc.*, 2014, **136**, 15054-15064.
46. N. Feng, P. He and H. Zhou, *ChemSusChem*, 2015, **8**, 600-602.
47. B. J. Bergner, M. R. Busche, R. Pinedo, B. B. Berkes, D. Schroder and J. Janek, *ACS Appl. Mater. Interfaces*, 2016, **8**, 7756-7765.
48. Q. C. Liu, J. J. Xu, S. Yuan, Z. W. Chang, D. Xu, Y. B. Yin, L. Li, H. X. Zhong, Y. S. Jiang, J. M. Yan and X. B. Zhang, *Adv. Mater.*, 2015, **27**, 5241-5247.
49. B. Liu, W. Xu, J. Tao, P. Yan, J. Zheng, M. H. Engelhard, D. Lu, C. Wang and J.-G. Zhang, *Adv. Energy Mater.*, 2018, **8**, 1702340.
50. L. Ye, M. Liao, H. Sun, Y. Yang, C. Tang, Y. Zhao, L. Wang, Y. Xu, L. Zhang, B. Wang, F. Xu, X. Sun, Y. Zhang, H. Dai, P. G. Bruce and H. Peng, *Angew. Chem. Int. Ed. Engl.*, 2019, **58**, 2437-2442.
51. X. Zhang, Q. Zhang, X. G. Wang, C. Wang, Y. N. Chen, Z. Xie and Z. Zhou, *Angew. Chem. Int. Ed. Engl.*, 2018, **57**, 12814-12818.
52. K. Liao, S. Wu, X. Mu, Q. Lu, M. Han, P. He, Z. Shao and H. Zhou, *Adv. Mater.*, 2018, e1705711.
53. M. Asadi, B. Sayahpour, P. Abbasi, A. T. Ngo, K. Karis, J. R. Jokisaari, C. Liu, B. Narayanan, M. Gerard, P. Yasaei, X. Hu, A. Mukherjee, K. C. Lau, R. S. Assary, F. Khalili-Araghi, R. F. Klie, L. A. Curtiss and A. Salehi-Khojin, *Nature*, 2018, **555**, 502-506.
54. Z. Huang, J. Ren, W. Zhang, M. Xie, Y. Li, D. Sun, Y. Shen and Y. Huang, *Adv. Mater.*, 2018, **30**, e1803270.
55. N. Togasaki, T. Momma and T. Osaka, *J. Power Sources*, 2015, **294**, 588-592.
56. Y. Yu, Y.-B. Yin, J.-L. Ma, Z.-W. Chang, T. Sun, Y.-H. Zhu, X.-Y. Yang, T. Liu and X.-B. Zhang, *Energy Storage Mater.*, 2019, **18**, 382-388.
57. W. Walker, V. Giordani, J. Uddin, V. S. Bryantsev, G. V. Chase and D. Addison, *J. Am. Chem. Soc.*, 2013, **135**, 2076-2079.
58. J. Uddin, V. S. Bryantsev, V. Giordani, W. Walker, G. V. Chase and D. Addison, *J. Phys. Chem. Lett.*, 2013, **4**, 3760-3765.
59. Rosy, S. Akabayov, M. Leskes and M. Noked, *ACS Appl. Mater. Interfaces*, 2018, **10**, 29622-29629.
60. T. Zhang, K. Liao, P. He and H. Zhou, *Energy Environ. Sci.*, 2016, **9**, 1024-1030.
61. B. Tong, J. Huang, Z. Zhou and Z. Peng, *Adv. Mater.*, 2018, **30**, 1704841.
62. B. Liu, W. Xu, P. Yan, X. Sun, M. E. Bowden, J. Read, J. Qian, D. Mei, C.-M. Wang and J.-G. Zhang, *Adv. Funct. Mater.*, 2016, **26**, 605-613.
63. N. Togasaki, T. Momma and T. Osaka, *J. Power Sources*, 2016, **307**, 98-104.
64. Q. Zhao, Y. Zhang, G. Sun, L. Cong, L. Sun, H. Xie and J. Liu, *ACS Appl. Mater. Interfaces*, 2018, **10**, 26312-26319.
65. H. Kim, T. Y. Kim, V. Roev, H. C. Lee, H. J. Kwon, H. Lee, S. Kwon and D. Im, *ACS Appl. Mater. Interfaces*, 2016, **8**, 1344-1350.
66. G. Huang, J. Han, C. Yang, Z. Wang, T. Fujita, A. Hirata and M. Chen, *NPG Asia Mate.*, 2018, **10**, 1037-1045.
67. D. J. Lee, H. Lee, Y. J. Kim, J. K. Park and H. T. Kim, *Adv. Mater.*, 2016, **28**, 857-863.
68. C. Zhao, J. Liang, Y. Zhao, J. Luo, Q. Sun, Y. Liu, X. Lin, X. Yang, H. Huang, L. Zhang, S. Zhao, S. Lu and X. Sun, *J. Mater. Chem. A*, 2019, **7**, 24947-24952.
69. Y. Yang, Q. Wu, Y. Cui, Y. Chen, S. Shi, R. Z. Wang and H. Yan, *ACS Appl. Mater. Interfaces*, 2016, **8**, 25229-25242.
70. S. Shi, J. Gao, Y. Liu, Y. Zhao, Q. Wu, W. Ju, C. Ouyang and R. Xiao, *Chinese Phys. B*, 2016, **25**, 018212.
71. S. Wang, J. Wang, J. Liu, H. Song, Y. Liu, P. Wang, P. He, J. Xu and H. Zhou, *J. Mater. Chem. A*, 2018, **6**, 21248-21254.
72. H. Kitaura and H. Zhou, *Chem. Commun. (Camb)*, 2015, **51**, 17560-17563.
73. H. Kitaura and H. Zhou, *Sci. Rep.*, 2015, **5**, 13271.
74. Y. Liu, B. Li, H. Kitaura, X. Zhang, M. Han, P. He and H. Zhou, *ACS Appl. Mater. Interfaces*, 2015, **7**, 17307-17310.
75. X. B. Zhu, T. S. Zhao, Z. H. Wei, P. Tan and L. An, *Energy Environ. Sci.*, 2015, **8**, 3745-3754.
76. D. Safanama and S. Adams, *J. Power Sources*, 2017, **340**, 294-301.
77. K. Zhang, S. Mu, W. Liu, D. Zhu, Z. Ding and Y. Chen, *Ionics*, 2018, **25**, 25-33.
78. J. Yi, S. Guo, P. He and H. Zhou, *Energy Environ. Sci.*, 2017, **10**, 860-884.
79. J. F. Wu, B. W. Pu, D. Wang, S. Q. Shi, N. Zhao, X. Guo and X. Guo, *ACS Appl. Mater. Interfaces*, 2019, **11**, 898-905.
80. J. Wang, Y. Yin, T. Liu, X. Yang, Z. Chang and X. Zhang, *Nano Res.*, 2018, **11**, 3434-3441.

81. H. T. T. Le, R. S. Kalubarme, D. T. Ngo, H. S. Jadhav and C.-J. Park, *J. Mater. Chem. A*, 2015, **3**, 22421-22431.
82. H. T. T. Le, D. T. Ngo, V.-C. Ho, G. Cao, C.-N. Park and C.-J. Park, *J. Mater. Chem. A*, 2016, **4**, 11124-11138.
83. H. T. T. Le, D. T. Ngo, P. N. Didwal, J. G. Fisher, C.-N. Park, I.-D. Kim and C.-J. Park, *J. Mater. Chem. A*, 2019, **7**, 3150-3160.
84. H. S. Jadhav, R. S. Kalubarme, A. H. Jadhav and J. G. Seo, *Electrochim. Acta*, 2016, **199**, 126-132.
85. X.-P. Zhang, Z.-Y. Wen and T. Zhang, *J. Mater. Chem. A*, 2018, **6**, 12945-12949.
86. S. Liu, W. Zhang, N. Chen and C. Sun, *ChemElectroChem*, 2018, **5**, 2181-2185.
87. S. Wu, Y. Qiao, H. Deng and H. Zhou, *J. Mater. Chem. A*, 2018, **6**, 9816-9822.
88. Z.-F. Chen, X. Lin, H. Xia, Y. Hong, X. Liu, S. Cai, J.-N. Duan, J. Yang, Z. Zhou, J.-K. Chang, M. Zheng and Q. Dong, *J. Mater. Chem. A*, 2019, **7**, 14260-14270.
89. K. Luo, G. Zhu, Y. Zhao, Z. Luo, X. Liu, K. Zhang, Y. Li and K. Scott, *J. Mater. Chem. A*, 2018, **6**, 7770-7776.
90. Y. Qiao, Y. He, S. Wu, K. Jiang, X. Li, S. Guo, P. He and H. Zhou, *ACS Energy Lett.*, 2018, **3**, 463-468.
91. D. Hirshberg, D. Sharon, E. De La Llave, M. Afri, A. A. Frimer, W. J. Kwak, Y. K. Sun and D. Aurbach, *ACS Appl. Mater. Interfaces*, 2017, **9**, 4352-4361.
92. F. Guo, T. Kang, Z. Liu, B. Tong, L. Guo, Y. Wang, C. Liu, X. Chen, Y. Zhao, Y. Shen, W. Lu, L. Chen and Z. Peng, *Nano Lett.*, 2019, **19**, 6377-6384.
93. W.-J. Kwak, H.-J. Shin, J. Reiter, N. Tsiouvaras, J. Hassoun, S. Passerini, B. Scrosati and Y.-K. Sun, *J. Mater. Chem. A*, 2016, **4**, 10467-10471.
94. H. Guo, G. Hou, D. Li, Q. Sun, Q. Ai, P. Si, G. Min, J. Lou, J. Feng and L. Ci, *ACS Appl. Mater. Interfaces*, 2019, **11**, 30793-30800.

Table of Contents

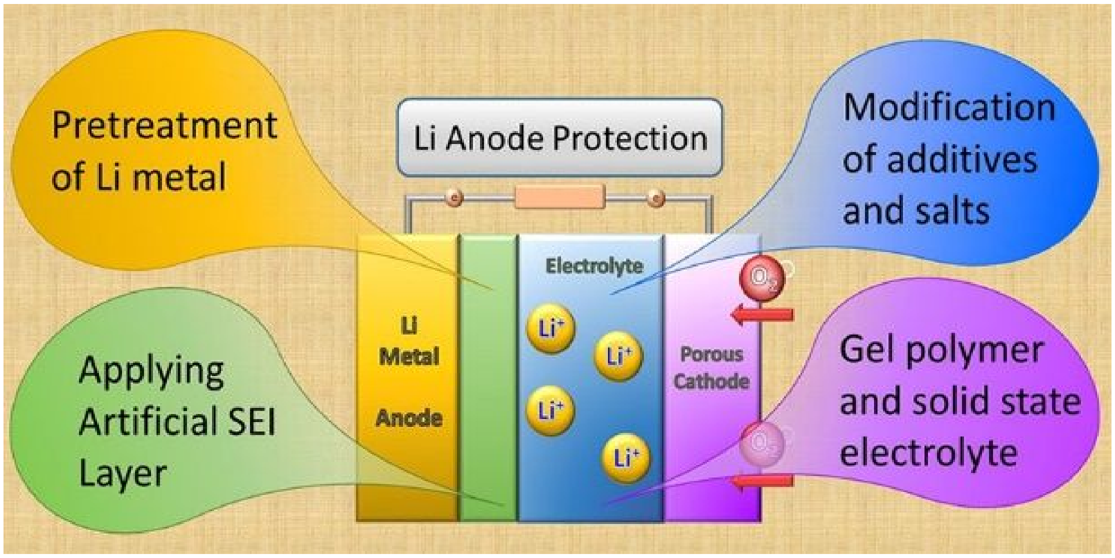

An overview is presented of the recent advances on Li anode protection in aprotic Li-O_2 batteries.